Research Article | Vol. 11, No. 1 / 1 January 2021 / Optical Materials Express 23

Optical Materials EXPRESS

Generalized hybrid anapole modes in all-dielectric ellipsoid particles [Invited]

ANAR K. OSPANOVA,[1,2] ALEXEY BASHARIN,[1,3,4] ANDREY E. MIROSHNICHENKO,[5] AND BORIS LUK'YANCHUK[6,*]

[1] *National University of Science and Technology "MISiS", The Laboratory of Superconducting Metamaterials and Department of Theoretical Physics and Quantum Technologies, Leninsky pr. 4, 119049, Moscow, Russia*
[2] *Department of Physics and Technology, al-Farabi Kazakh National University, 71 al-Farabi Av., 050040 Almaty, Kazakhstan*
[3] *Institute for Theoretical and Applied Electromagnetics RAS, 13 Izhorskaya, Moscow 125412, Russia*
[4] *Moscow Institute of Physics and Technology, Dolgoprudny, Moscow Region, 117303, Russia*
[5] *School of Engineering and Information Technology, UNSW Canberra, ACT 2600, Australia*
[6] *Faculty of Physics, Lomonosov Moscow State University, Moscow, 119991, Russia*
[*] *lukiyanchuk@nanolab.phys.msu.ru*

Abstract: Numerous exciting optical effects in all-dielectric high-refractive-index structures are associated with so-called toroidal electrodynamics. Among these effects are anapoles, nonradiated states caused by interference phenomena, e.g. between electric dipole and toroidal dipole modes. For a spherical particle it is possible to reach simultaneous destructive interference for electric, magnetic, and corresponding toroidal dipole modes (so-called hybrid anapole mode), by varying the refractive index and/or particle size. However, there are no sufficient degrees of freedom within spherical geometry to extend the hybrid anapole mode effect to higher multipoles. Due to the optical theorem, it is also impossible to create the ideal anapole with destructive interference for all multipoles under plane wave illumination. In principle, it is possible to suppress radiation losses for the finite number of multipoles only by constructing the nanoantenna with complex geometry. Our approach of the hybrid anapole state excitation, we demonstrate in ellipsoidal all-dielectric particle providing cancellation of both electric and magnetic scattering up to quadrupole modes. This effect is achieved due to the optimised geometry of the ellipsoidal particle. Moreover, we provide classification of novel anapoles arising due to interference between moments and their mean- square radii (MSR) of electric, magnetic and toroidal family and introduce generalized anapoles for high order interaction between moments. Our concept is useful for the design of light controlling devices, reflectionless metasurfaces, high Q-factor opened resonators and nonscattering particle development.

1. Introduction

There are two long-standing problems in nanophotonics and laser-matter interaction [1]. The first one is related to the creation and analysis of field distributions at scales much shorter than the radiation wavelength. This problem is in the foundation of the novel photonic technologies including nanoantennas, biosensing/detecting devices, beam splitting and cloaking. The second problem is related to the possibility of creating a high-quality open resonator with a Q-factor comparable to the reciprocal of the natural linewidth of an excited atom, $Q=\omega/\Delta\omega$. This is quite challenging for nanometer-scale structures. According to the whispery gallery modes (WGM) theory [2] the interface with a curvature (as in the case of the sphere), does not support the total internal reflection: part of the wave still seeps out of the ball out. This leakage can be small just for sufficiently large structures. Small structures, in general, have strong radiation losses. It limits the efficiency of nanolasers as well as an electric and magnetic intensities at the nanoscale. In

#414340
Journal © 2021
https://doi.org/10.1364/OME.414340
Received 5 Nov 2020; accepted 23 Nov 2020; published 4 Dec 2020

recent years, however, the hope has arisen that both problems can be solved within the framework of toroidal electrodynamics [3].

Note, that even possibility of directional scattering for nanoparticles is quite challenging, because of symmetrical Rayleigh dipole scattering. However, it can be broken for perfectly conducting nanoparticles, where the ratio of forward and backward scattering intensities is equal to 1:9 [4]. Another ability is related to plasmonic nanoparticles, which have a fast variation of the forward scattering to backward scattering near quadrupole resonance [5]. It is also possible to realize in high refractive index nanoparticles which possess strong magnetic response [6,7]. It was shortly confirmed experimentally [8,9]. Ability to control strong magnetic and electric dipoles yields a wealth of unique optical properties. For example, at the frequency of radiation where the amplitudes and phases of magnetic and electric dipoles are equal (it is the so-called the first Kerker condition [10]) the backward scattering is completely suppressed in the dipole approximation [11–13]. All-dielectric resonant nanostructures have emerged as a promising platform for many nanophotonics applications, see e.g. [14–16]. In contrast, the anapole mode (this term was introduced by Ya. Zeldovich [17]) are characterized by the zero scattering in all possible directions, that is, about complete invisibility in the far-field. Interestingly, this does not prevent the object from being visible in the near-field. It was observed experimentally in the microwave with metamaterial which unit cell, containing four split wire loops embedded into a dielectric slab [18], as well as in optical range with silicon nanocylinders [19], in plasmonics [20] and many other systems [21–40].

2. Classification of anapoles

Scattering of the plane monochromatic wave by the dielectric particle is described by a solution of Maxwell equations together with boundary conditions. Analysis of this solution is based on the multipolar decomposition [41–44], which indicates the correspondence between the multipolar components of the source and the multipolar fields radiated by it. This multipolar decomposition can be done in different ways, e.g. by using spherical multipoles or Cartesian moments [43,44]. The Cartesian approach is more suitable for introducing of the toroidal moment [45].

Although, the anapole represents a specific example of interference effect arises from the interaction of three families of multipolar modes: electric, magnetic, and toroidal [46]. However, the well-known electric anapole mode is caused by destructive interference of electric dipole and toroidal dipole mode [18–36,47,48].

In addition, the technique for magnetic anapole mode excitation analytically studied in extremely high-index all-dielectric spherical particles [49]. The mechanism for such magnetic nonradiating state is different from electric anapole excitation and aimed at extinguishing magnetic response utilizing excitation of so-called magnetic mean square radii moments (MSR) interfering with a magnetic dipole moment. On the other hand, one can pursue the idea of coexistence of both electric and magnetic anapole modes for creation of purely nonradiating sources, also known as hybrid anapole [49]. The main advantage of hybrid anapole is that the scattering cross section of electric and magnetic multipoles tends to zero and hybrid anapole supporting by particle appears invisible.

Indeed, the scattering cross section of the particle can be described by terms of multipoles [50]:

$$\sigma_{scat} = 2\frac{\sqrt{\frac{\mu_0}{\varepsilon_0\varepsilon_p}}}{|\boldsymbol{E}_{inc}|^2}\left\{\frac{k^4\sqrt{\varepsilon_p}}{12\pi\varepsilon_0{}^2c\mu_0}\left|p_i+\frac{ik\varepsilon_p}{c}T_i+\frac{ik^3\varepsilon_p{}^2}{c}T_i^{\langle 2\rangle}\right|^2\right.$$
$$\left.+\frac{k^4\varepsilon_p\sqrt{\varepsilon_p}}{12\pi\varepsilon_0 c}\left|m_i+\frac{ik\varepsilon_p}{c}M_i^{\langle 2\rangle}\right|^2+\frac{k^6\varepsilon_p\sqrt{\varepsilon_p}}{160\pi\varepsilon_0{}^2c\mu_0}\left|Q_{ij}^e+\frac{ik\varepsilon_p}{c}Q_{ij}^T\right|^2+\frac{k^6\varepsilon_p{}^2\sqrt{\varepsilon_p}}{160\pi\varepsilon_0 c}\left|Q_{ij}^m+\frac{ik\varepsilon_p}{c}Q_{ij}^{m\,\langle 2\rangle}\right|^2\dots\right\} \tag{1}$$

Optical Materials EXPRESS

Here ε_0 and μ_0 are vacuum permittivity and permeability, ε_p - permittivity of the surrounding medium c - speed of light, k - wavenumber, $\boldsymbol{E}_{in}$ - is the amplitude of an incident $\boldsymbol{E}$ -field. We use Cartesian multipole expansion, where p_i - electric dipole, m_i - magnetic dipole, T_i - toroidal dipole, $M_i^{\langle 2\rangle}$-magnetic so-called mean-square radii, $T_i^{\langle 2\rangle}$ - toroidal mean-square radii, Q_{ij}^e-electric quadrupole, Q_{ij}^m - magnetic quadrupole, Q_{ij}^T-toroidal quadrupole moments and $Q_{ij}^{m\langle 2\rangle}$ - mean-square radius of magnetic quadrupole. Omitted octupole terms and corresponding toroidal moments can be found in Ref. [44,46,50–52]. All multipole modes are expressed by integrals over particle volume with different moments of current j [50].

Dipole moments:

$$\begin{aligned} p_i &= \frac{i}{\omega}\int_V j_i d^3r \\ m_i &= \frac{1}{2}\int_V (\boldsymbol{r}\times\boldsymbol{j})_i d^3r \qquad , \\ T_i &= \frac{1}{10}\int_V [(\boldsymbol{j}\cdot\boldsymbol{r})r_i - 2r^2 j_i]d^3r \end{aligned} \tag{2}$$

Quadrupole moments:

$$\begin{aligned} Q_{ij}{}^e &= \frac{i}{\omega}\int_V [r_i j_j + r_j j_i - \frac{2}{3}\delta_{ij}(\boldsymbol{r}\cdot\boldsymbol{j})r_i]d^3r \\ Q_{ij}{}^m &= \frac{1}{3}\int_V [(\boldsymbol{r}\times\boldsymbol{j})_i r_j + (\boldsymbol{r}\times\boldsymbol{j})_j r_i]d^3r \\ Q_{ij}{}^T &= \frac{1}{42}\int_V [4(\boldsymbol{r}\cdot\boldsymbol{j})r_i r_j + 2(\boldsymbol{j}\cdot\boldsymbol{r})r^2\delta_{ij} - 5r^2(r_i j_j + r_j j_i)]d^3r \end{aligned} \tag{3}$$

Mean-square radii:

$$\begin{aligned} M_i{}^{\langle 2\rangle} &= \frac{i\omega}{20}\int_V r^2(\boldsymbol{r}\times\boldsymbol{j})_i d^3r \\ T_i{}^{\langle 2\rangle} &= \frac{1}{280}\int_V [3r^4 j_i - 2r^2(\boldsymbol{r}\cdot\boldsymbol{j})rj_i]d^3r \\ Q_{ij}{}^{m\langle 2\rangle} &= \frac{i\omega}{42}\int_V r^2[(\boldsymbol{r}\times\boldsymbol{j})_i r_j + (\boldsymbol{r}\times\boldsymbol{j})_j r_i]d^3r \end{aligned} \tag{4}$$

Although one can be confused about the definition of anapoles, but we introduce a classification and define generalized conditions for anapoles (Table 1).

Table 1. Classification of anapoles

No	Type	Trivial	Nontrivial
1	Electric anapole		$p_i = -\frac{ik\varepsilon_p}{c}T_i$
2	Magnetic anapole	$m_i = -\frac{ik\varepsilon_p}{c}M_i^{\langle 2\rangle}$	
3	Toroidal anapole	$T_{i=} - ik^2\varepsilon_p T_i^{\langle 2\rangle}$	$p_i = -\frac{ik^3\varepsilon_p{}^2}{c}T_i^{\langle 2\rangle}$
4	Electric quadrupole anapole		$Q_{ij}^e = -\frac{ik\varepsilon_p}{c}Q_{ij}^T$
5	Magnetic quadrupole anapole	$Q_{ij}^m = -\frac{ik\varepsilon_p}{c}Q_{ij}^{m\langle 2\rangle}$	

At this point, we can distinguish the *trivial* anapoles which are the result of interaction between multipoles and their MSR of the same families, and *nontrivial anapoles*, which in contrast, can be excited by multipoles of different families. The most famous *electric anapole* (1 in Table 1) is nontrivial nonradiating configuration, while destructive interference between electric and toroidal quadrupoles produces nontrivial *electric quadrupole anapole* (4 in Table 1) of next order. Destructive interference between magnetic moment and magnetic MSR moment provides trivial *magnetic anapole* (2 in Table 1) configuration [41–44]. Hybrid anapole of both electric

Optical Materials EXPRESS

and magnetic anapole excitations suppress scattering of electric and magnetic origin. Since the theory of hybrid anapoles have emerged quite recently, there are a just few works on its theoretical investigation [49].

Moreover, the first term in Eq. (1) shows that toroidal MSR contributes to total electric anapole and condition $p_i + \frac{ik\varepsilon_p}{c}T_i + \frac{ik^3{\varepsilon_p}^2}{c}T_i^{\langle 2\rangle} = 0$ should be satisfied. In additional, to the classical electrical anapole, two extra destructive interactions appear in the system.

Toroidal anapole (3 in Table 1) appears to be in both nontrivial and trivial states. Indeed, interaction in destructive manner of toroidal moment and its MSR is trivial due to interference between dipoles of the same family. In contrast, nontrivial toroidal anapole can be emerged due to interaction of electric dipole moment with toroidal MSR.

Magnetic quadrupole anapole is trivial configuration of interacting of magnetic quadrupole with its mean square radius (5 in Table 1).

From Table 1, we can expect that trivial and nontrivial anapole configurations excited in particle by external radiation lead to invisibility due to almost suppressed scattering (1) provided by several anapole types in the same frequency range.

In general, higher-order multipole modes produce lower scattering. Thus, providing conditions for the suppression of four main terms in Eq. (1) we expect a high level of invisibility in the same frequency range. Note, that even with excitation of electric anapole it is possible to reach scattering below the Rayleigh scattering [25].

Moreover, in Table 2 we show four *generalized anapole* modes which we intend excite simultaneously in hybrid anapole mode and demonstrate their contribution to the far-field. These modes correspond to four attendants in Eq. (1). The first term in Eq. (1) shows that toroidal moment and its MSR contributes to total electric dipole. For complete invisibility, we need to combine not only trivial and also nontrivial anapole modes to reach the total suppression for the electric and magnetic radiation (Table 2).

Table 2. Generalized anapole conditions

No	Type	Short	Anapole mode
1	Generalized electric dipole	ed	$p_i + \frac{ik\varepsilon_p}{c}T_i + \frac{ik^3{\varepsilon_p}^2}{c}T_i^{\langle 2\rangle}$
2	Generalized magnetic dipole	md	$m_i + \frac{ik\varepsilon_p}{c}M_i^{\langle 2\rangle}$
3	Generalized electric quadrupole	eq	$Q_{ij}^e + \frac{ik\varepsilon_p}{c}Q_{ij}^T$
4	Generalized magnetic quadrupole	mq	$Q_{ij}^m + \frac{ik\varepsilon_p}{c}Q_{ij}^{m\langle 2\rangle}$

The problem, however, is that we need a sufficient number of free parameters to provide suppression of the corresponding modes. For example, for spherical particle it is possible to provide suppression of both electric and magnetic dipole modes by a selection of two free parameters in the Mie theory: refractive index $n = \sqrt{\varepsilon_p}$ and size parameter $q{=}2\pi R/\lambda$ (R is radius of the particle). It is impossible to provide suppression of all dipole and quadrupole scattering for spherical particle simultaneously. However, by changing the particle geometry one can acquire additional free parameter, e.g. the ratio of the major semi-axis a to the minor semi-axis b (i.e., the aspect ratio a/b) characterizes the spheroidal (ellipsoid of revolution) particle shape [53]. In Ref. [53] this additional parameter was used to provide for oblate (disk-like shape) spheroid *maximum forward light scattering* together with suppression of backscattering due to the first Kerker condition. In principle, one can use this additional parameter to find *minimum forward scattering* together with suppression of backscattering for spheroid. However, for spheroid, we can suppress only one – electric or magnetic quadrupole scattering mode.

Optical Materials EXPRESS

To suppress both quadrupole scattering modes, we heed two additional free parameters, e.g. using three axes in parallelepiped ($a \times b \times \bar{c}$) or 3D ellipsoid particle with shape given by equation

$$\frac{x^2}{a^2} + \frac{y^2}{b^2} + \frac{z^2}{\bar{c}^2} = 1 \tag{5}$$

In this paper, we demonstrate the theoretical model based on the all-dielectric 3D ellipsoid particle (see in Fig. 1), which scatter the plane wave in hybrid anapole manner. Therefore, we endeavor to show the tunability of different type of anapoles in ellipsoid particle by the interplay of its geometrical parameters, which may indicate on physical nature of the multipole as a whole.

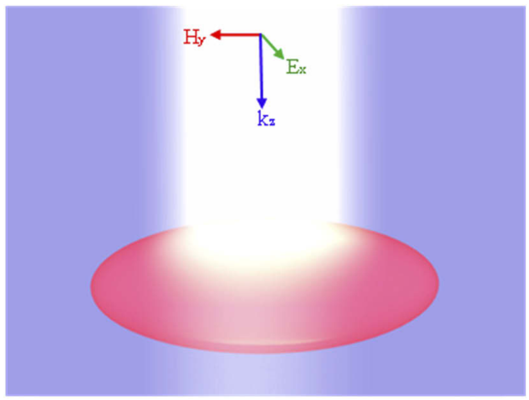

Fig. 1. Illustration of an all-dielectric ellipsoidal particle placed on the vacuum medium. Wavevector **k** is directed along z-axis and electric field **E** directed along x-axis.

The study of ellipsoidal structures is important not only for invisible nanophotonics applications but also for investigations of large astrophysical objects. Many particles in planetary and interstellar dust are crystalline of nonspherical – ellipsoidal shape; therefore, understanding their scattering characteristics may be useful in inverse-scattering astrophysical and aerosol problems [52–57]. Probably, the study of the invisible properties of ellipsoidal objects will be able to explain the nature of these objects.

3. Results and discussion

In order to demonstrate generalized hybrid anapole approach we perform numerical simulation of electromagnetic scattering by ellipsoidal particle by a commercial version of CST Microwave Studio and using *Time domain solver* with open boundary conditions. The particle is illuminated by a plane wave (Fig. 1).

The parameters of the particle are as follows: the major axis is b=*1.85R* the minor axes are a=*0.7R* and $c = R$, dielectric permittivity is ε_p=*30*. An external linearly polarized wave incident on the ellipsoidal particle in normal direction so that wavevector is co-directed with minor axis $\bar{c}$. Another minor axis a corresponds to the electric component and major axis b, respectively, corresponds to the magnetic component of the wave.

We characterize the electromagnetic response of particle by the scattering cross section spectrum (Fig. 2). We observe almost zero scattering at q=0.85, which implies that the nonradiating state of the particle is excited, where both generalized dipole modes and electric quadrupole mode are suppressed. We plot scattering cross section via independent parameter $q = 2\pi R/\lambda$ and normalized on ellipse cross-section $S = \pi ab$. The total scattering is limited by magnetic quadrupole mode. However, the scattering beyond this range is very high ~ 10.

Optical Materials EXPRESS

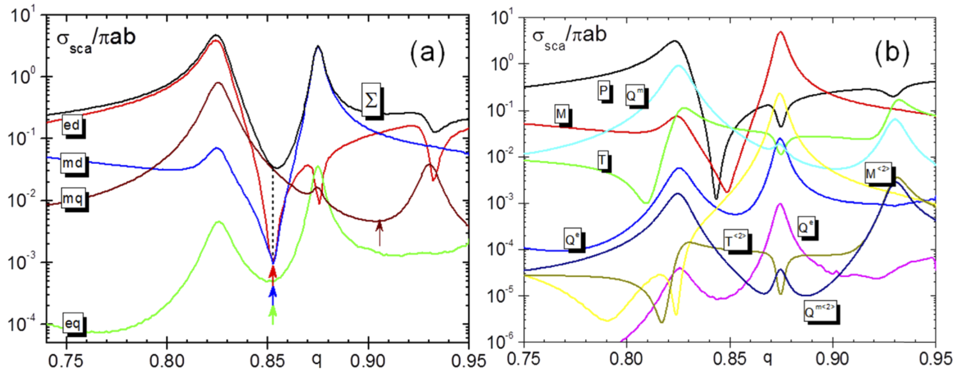

Fig. 2. Scattering cross section and contribution of basic multipoles in Table 1(a)- Electric dipole contribution ("ed" first term in Eq. (1)) – red line. Magnetic dipole contribution ("md" second term in Eq. (1)) – blue line. Electric quadrupole contribution ("eq" third term in Eq. (1)) – green line. Magnetic quadrupole contribution ("mq" fourth term in Eq. (1)) – wine line. Sum of four terms – black line. (b)- p - electric dipole, m - magnetic dipole, T - toroidal dipole, $M^{<2>}$ -magnetic so-called mean-square radii, $T^{<2>}$ - toroidal mean-square radii, Q^e- electric quadrupole, Q^m- magnetic quadrupole, Q^T -toroidal quadrupole moments and $Q^{m<2>}$- mean-square radius of magnetic quadrupole.

Therefore, it is proved by near field distribution maps at this frequency, demonstrating unperturbed wavefront propagation through the particle (Fig. 3(a, b and c) for electric field and d, e, f for magnetic field). Thus, the particle at frequency $q = 0.85$ is implied to be invisible. We were not able to reach simultaneously local minimum for magnetic quadrupole, which is situated at higher frequencies, $q = 0.91$. However, this magnetic quadrupole mode can also be suppressed for the particle on the substrate as it is shown further.

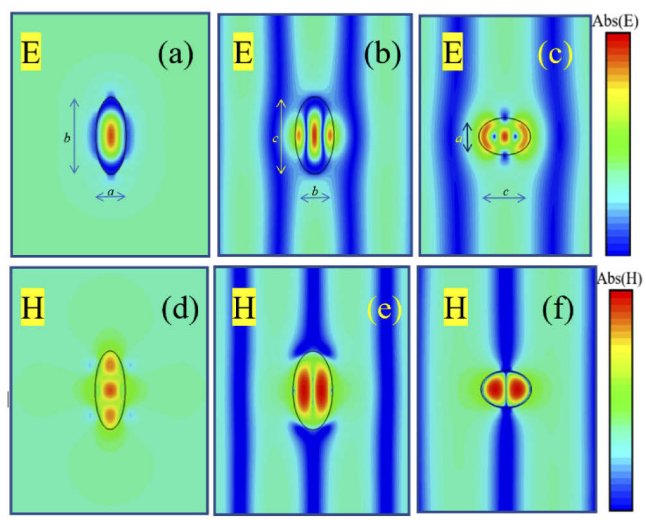

Fig. 3. Electric and magnetic fields distribution in xy-plain (a, d), yz-plain (b, e), and zx-plain (c, f) of ellipsoid particle with axis: a=$0.7R$, b=$1.85R$ and $c = R$ at $q = 0.85$.

For considered particle parameters, one can see resonant behavior of multipoles intensities at $q = 0.85$, their dipole moments and quadrupole, as well as mean-square radii. Namely, the interference of electric type dipoles, i.e. electric and toroidal dipoles, as well as toroidal MSR (see, the red curve in Fig. 2) perfectly coincides with the position of interference of magnetic type dipoles – magnetic dipole and magnetic MSR (see, blue curve in Fig. 4(a)). Therefore, these suppressed intensities are accompanied by deep-lying (10^{-3}) electric type quadrupoles (electric and toroidal quadrupoles, see, the green curve in Fig. 4(a)). The intensity of magnetic type quadrupoles (magnetic quadrupole and MSR of magnetic quadrupole) is nearly zero (0.02) and exceeds other kinds of multipoles. However, it does not strongly affect no scattering pattern of the particle.

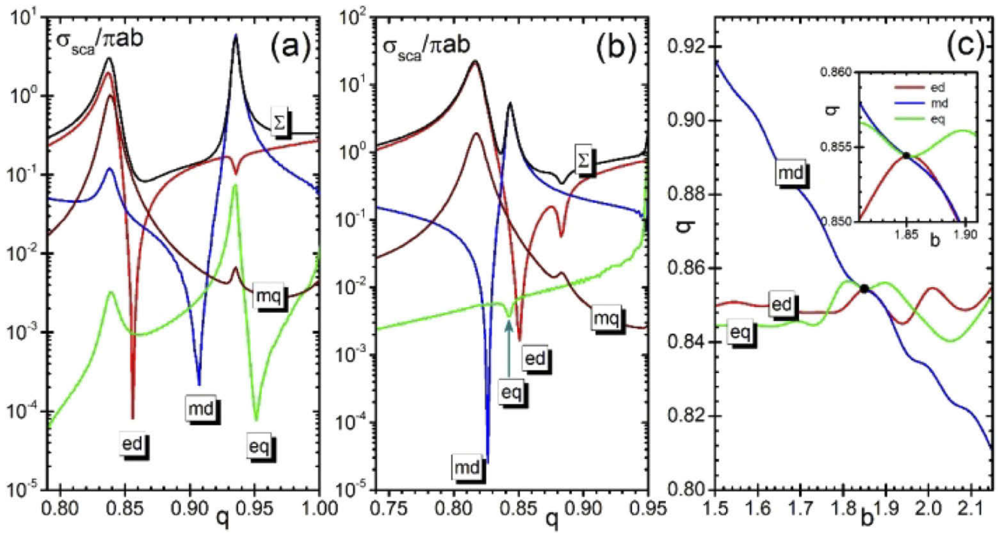

Fig. 4. Intensities of interfering anapoles of dipole and quadrupole orders for the ellipsoid of parameter a=0.7R, b=1.55R and $c = R$ (a) and $b = 2.05R$ (b), (c)- evaluation of anapoles with b.

As for an individual contribution of each multipole, the overlap between electric and magnetic moments and their mean square radii is observed at $q = 0.85$ (see, Fig. 2(b)). Although, toroidal and electric moments coincide in intensities at $q = 0.85$ forming electric anapole, while magnetic moment interferes destructively with magnetic MSR forming magnetic anapole. The similar regime is observed for electric quadrupole anapoles. As a total, the contribution of three types of anapoles of electric, magnetic, and electric quadrupole anapoles constitutes *hybrid anapole* at $q = 0.85$.

However, we must clarify the qualitative resonant coincidence of various types of anapoles forming a hybrid anapole. For this aim, we demonstrate how each parameter governs multipoles positions and enables physically tuning of their anapoles. In particular, the changing of major axis b leads to the detuning of hybrid anapole state with widespread of multipoles, see Fig. 4. Namely, lessening (elongating) of the major axis b leads to the redshift (blueshift) of magnetic anapole (blue curve) while electric anapole (red curve) stay around the same position, see Fig. 4(a) and (b). The same regime occurs for electric quadrupole anapole (green curve). Here, we conclude that the major axis b is a channel for *magnetic dipoles* tuning.

In order to estimate the evolution of anapoles frequencies with parameter b, we plot a graph of electric, magnetic, and electric quadrupole anapoles resonance frequencies depended on b parameter. Indeed, electric anapole and electric quadrupole anapole are almost unchanged during b variation. However, magnetic anapole frequency is changing dramatically with b from 1.5R to 2.2R (Fig. 4(c)).

Furthermore, we study the influence of the minor axis c, which is in the same direction wavevector of the external wave. In contrast with the situation above, the lessening (elongating)

Optical Materials EXPRESS

of the minor axis c leads to the blueshift (redshift) of electric anapole (red curve), while magnetic anapole (blue curve) and electric quadrupole anapole (green curve) stays almost unperturbed (Fig. 5(a) and (b)). Thus, minor axis c along wavevector can be defined as the channel for electric anapole tuning.

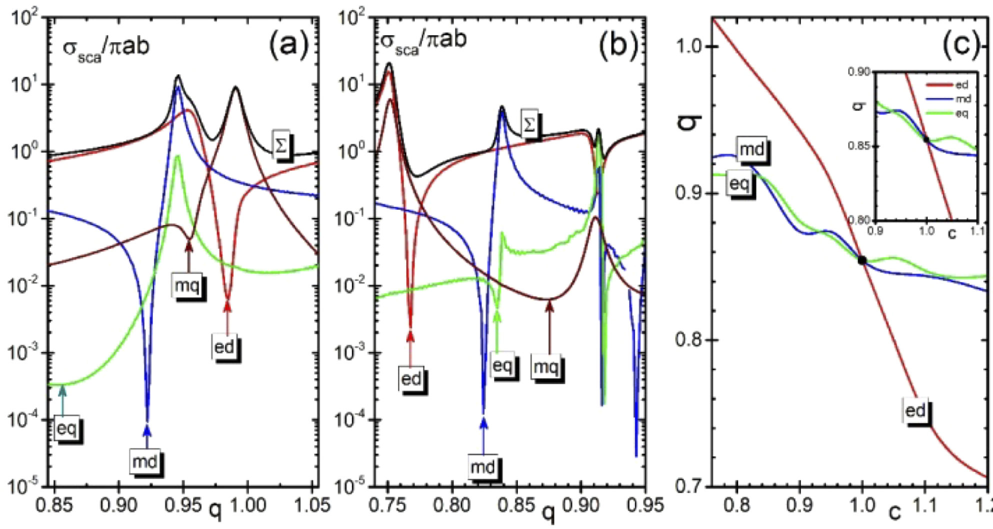

Fig. 5. Intensities of interfering multipoles of dipole and quadrupole orders for ellipsoid of parameter $a = 0.7R$, $b = 1.85R$ with $c = 0.75R$ (a) and $c = 1.2R$ (b), (c)- evaluation of anapoles with c.

We summarize the evaluation of anapoles with changing parameter c on the graph, which clearly demonstrates geometrical tunability of *electric anapole* (Fig. 5(c)).

The minor axis a is the tunable channel of *electric quadrupole anapole*. The resonance frequency of this type of anapole undergoes redshift with increasing a from $0.45R$ up to $0.85R$. However, this tunability is characterized by blueshift of a higher than $0.85R$ as soon as the ellipsoidal form of the particle becomes spheroidal if a tends to c (Fig. 6).

It is obvious from the previous discussion of Fig. 4–6, the parameters tuning enables suppression of scattering of electric and magnetic anapoles, as well as electric quadrupole anapole. Once the electric quadrupole anapole scattering is suppressed, magnetic quadrupoles scattering contribution becomes strong. On the one hand, in practical issues, the application of suitable low dielectric substrate may suppress this magnetic quadrupole response and, therefore, makes the realization of ideal hybrid nonradiating anapole one step closer.

Indeed, we intentionally do not present the magnetic quadrupole anapole on Fig. 4–6 since its contribution has not resonance frequency in the considered range. However, in real experiments, the ellipsoidal particle should be placed on the low-index substrate. Indeed, the Fabry–Pérot resonance arising due to multiple scattering from substrate borders enhances magnetic quadrupole moment of the particle, which is parasitic factor in many experiments of toroidal dipole observation in planar metamaterials [58]. But in our case, the substrate may play a positive role for suppression of magnetic quadrupole intensity in a destructive manner. Very recently, the role of Fabry–Pérot resonance in hybrid anapole excitation has been predicted for all-dielectric large cylinders [59].

For this aim, we consider our particle on a thin substrate with low permittivity of 1.5 and demonstrate how the magnetic quadrupole moment is interfering with MSR of magnetic quadrupole depending on substrate thickness (Fig. 7). For thinnest substrate $h = 0.2R$ (Fig. 7(a)) magnetic quadrupole anapole has not pronounced deep, but we observe strong its minima on $h = R$ and higher (Fig. 7(b) and (c)), where magnetic quadrupole anapole has intensity lower than

Optical Materials EXPRESS

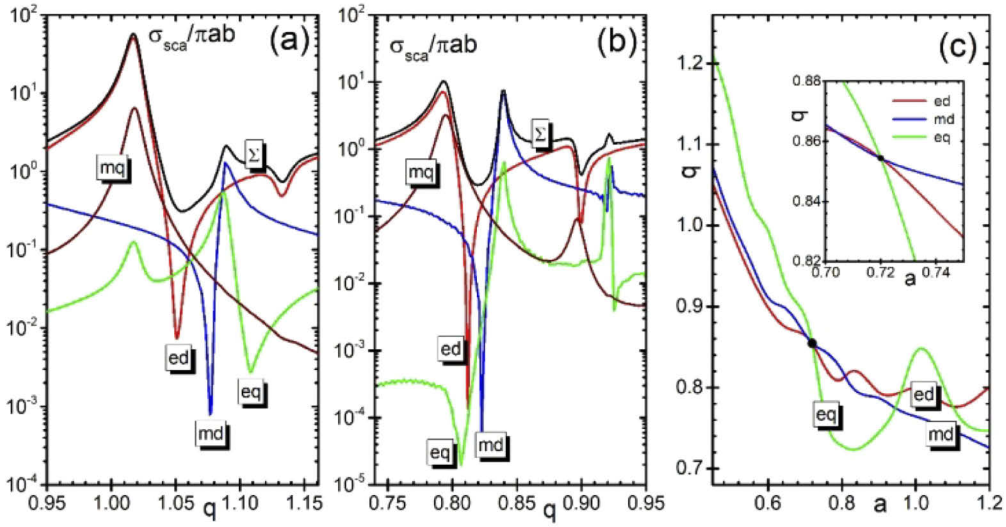

Fig. 6. Intensities of interfering multipoles of dipole and quadrupole orders for ellipsoid of parameter $c = R$, $b = 1.85R$ with $a = 0.45R$ (a), $a = 0.8R$ (b), (c) - evaluation of anapoles with a.

other anapoles. Thus, the fourth channel of magnetic quadrupole anapole complements hybrid anapole of the particle that closer to total invisibility of the particle.

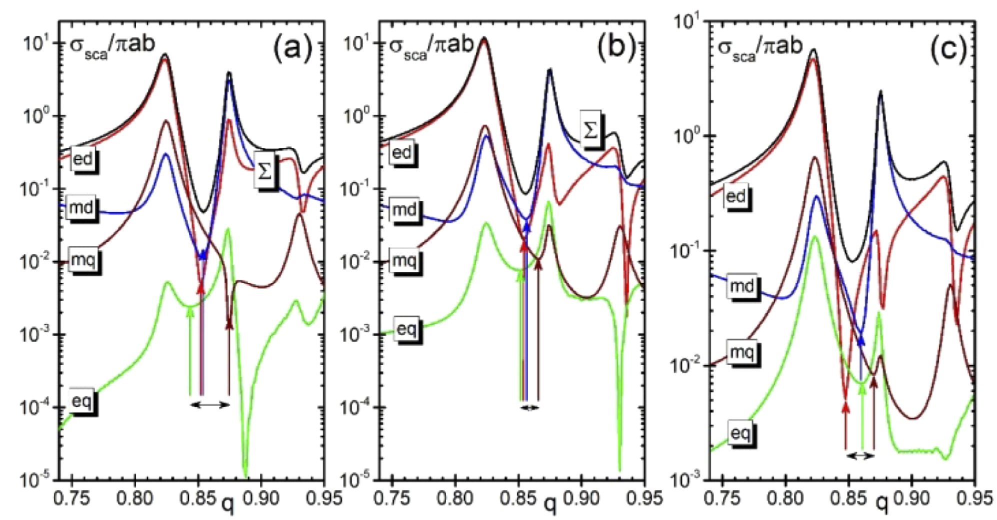

Fig. 7. Intensities of interfering multipoles of dipole and quadrupole orders for ellipsoid of parameter $a = 0.7R$, $c = R$, $b = 1.85R$ put on substrate of ε=1.5 with the thickness $h = 0.2R$ (a), R (b) and $1.8R$ (c).

As a summary, we should note, that ellipsoidal shape is closest to the shape of drops, which often arise during the fabrication of polymeric and eutectic micro and nanoparticles [58–65].

In particular, eutectic elliptical particles can be used for photonics where these materials have plasma frequency in THz range due to phonon- polariton interaction with high permittivity [66–70]. Moreover, the latest report of the demonstration of high-order anapole state in gold

Optical Materials EXPRESS

spheroids brings our concept of generalized hybrid anapoles in ellipsoidal particles to a new level [70].

4. Conclusion

In conclusion, we proposed classification of novel trivial and nontrivial anapoles arising due to interference between moments and their mean square radii (MSR) of electric, magnetic and toroidal family and introduce generalized anapoles for high order interaction between moments. We theoretically studied a novel class of all-dielectric ellipsoidal particle that exhibits a resonant hybrid anapole response. We demonstrated excitation by means of four generalized anapole channels which can be "manually" tuned by changing of axes of the ellipsoid and presented substrate. This particle possesses almost zero scattering due to electric, magnetic and their quadrupoles anapoles excitation. This technique can be promising for practical realization of invisible nanophotonics and strong field localization devices.

Funding

Australian Research Council; Russian Foundation for Basic Research (20-02-00715); Russian Science Support Foundation (20-12-00389, 20-72-00016); Ministry of Science and Higher Education of the Russian Federation (14.W03.31.0008).

Acknowledgments

This work was supported by Ministry of Science and Higher Education of the Russian Federation (grant 14.W03.31.0008). This work was partially supported by the Russian Science Foundation (No. 20-12-00389). The classification of anapoles and multipole decomposition was supported by Russian Science Foundation (No. 20-72-00016) The reported study was funded by RFBR, project number 20-02-00715. The work of AEM was supported by the Australian Research Council.

Disclosures

The authors declare no conflicts of interest.

References

1. L. Novotny and B. Hecht, *Principles of Nano-optics* (Cambridge University Press, 2012).
2. D. V. Strekalov, C. Marquardt, A. B. Matsko, H. G. Schwefel, and G. Leuchs, "Nonlinear and quantum optics with whispering gallery resonators," J. Opt. **18**(12), 123002 (2016).
3. N. Papasimakis, V. A. Fedotov, V. Savinov, T. A. Raybould, and N. I. Zheludev, "Electromagnetic toroidal excitations in matter and free space," Nat. Mater. **15**(3), 263–271 (2016).
4. L. D. Landau, E. M. Lifshitz, and L. P. Pitaevskii, "Electrodynamics of continuous media," Problem 2 to §92 (Butterworth-Heinemann, 2002).
5. B. Luk'yanchuk, N. I. Zheludev, S. A. Maier, N. J. Halas, P. Nordlander, H. Giessen, and T. C. Chong, "The Fano resonance in plasmonic nanostructures and metamaterials," Nat. Mater. **9**(9), 707–715 (2010).
6. A. B. Evlyukhin, C. Reinhardt, A. Seidel, B. Luk'yanchuk, and B. N. Chichkov, "Optical response features of Si-nanoparticle arrays," Phys. Rev. B **82**(4), 045404 (2010).
7. A. Garcia-Etxarri, R. Gomez-Medina, L. S. Froufe-Perez, C. Lopez, L. Chantada, F. Scheffold, J. Aizpurua, M. Nieto-Vesperinas, and J. J. Sáenz, "Strong magnetic response of submicron silicon particles in the infrared," Opt. Express **19**(6), 4815–4826 (2011).
8. A. I. Kuznetsov, A. E. Miroshnichenko, Y. H. Fu, J. B. Zhang, and B. Luk'yanchuk, "Magnetic light," Sci. Rep. **2**(1), 492 (2012).
9. A. B. Evlyukhin, S. M. Novikov, U. Zywietz, R. L. Eriksen, C. Reinhardt, S. I. Bozhevolnyi, and B. N. Chichkov, "Demonstration of magnetic dipole resonances of dielectric nanospheres in the visible region," Nano Lett. **12**(7), 3749–3755 (2012).
10. M. Kerker, D.-S. Wang, and C. L. Giles, "Electromagnetic scattering by magnetic spheres," J. Opt. Soc. Am. **73**(6), 765 (1983).

Optical Materials EXPRESS

11. J. M. Geffrin, B. García-Cámara, R. Gómez-Medina, P. Albella, L. S. Froufe-Pérez, C. Eyraud, A. Litman, R. Vaillon, F. González, M. Nieto-Vesperinas, J. J. Sáenz, and F. Moreno, "Magnetic and electric coherence in forward- and back-scattered electromagnetic waves by a single dielectric subwavelength sphere," Nat. Commun. **3**(1), 1171 (2012).
12. Y. H. Fu, A. I. Kuznetsov, A. E. Miroshnichenko, Y. F. Yu, and B. Luk'yanchuk, "Directional visible light scattering by silicon nanoparticles," Nat. Commun. **4**(1), 1527 (2013).
13. S. Person, M. Jain, Z. Lapin, J. J. Sáenz, G. Wicks, and L. Novotny, "Demonstration of zero optical backscattering from single nanoparticles," Nano Lett. **13**(4), 1806–1809 (2013).
14. A. I. Kuznetsov, A. E. Miroshnichenko, M. L. Brongersma, Y. S. Kivshar, and B. Luk'yanchuk, "Optically resonant dielectric nanostructures," Science **354**(6314), aag2472 (2016).
15. R. Paniagua-Domínguez, B. Luk'yanchuk, A. Miroshnichenko, and J. A. Sánchez-Gil, "Dielectric nanoresonators and metamaterials," J. Appl. Phys. **126**(15), 150401 (2019).
16. R. Paniagua-Dominguez, B. Luk'yanchuk, and A. I. Kuznetsov, "Control of scattering by isolated dielectric nanoantennas," in *Dielectric Metamaterials* (Woodhead Publishing, 2020), pp. 73–108.
17. Y. B. Zel'dovich, "Electromagnetic interaction with parity violation," Sov. Phys. JETP **6**, 1184–1186 (1958).
18. T. Kaelberer, V. A. Fedotov, N. Papasimakis, D. P. Tsai, and N. I. Zheludev, "Toroidal dipolar response in a metamaterial," Science **330**(6010), 1510–1512 (2010).
19. A. E. Miroshnichenko, A. B. Evlyukhin, Y. F. Yu, R. M. Bakker, A. Chipouline, A. I. Kuznetsov, B. Luk'yanchuk, B. N. Chichkov, and Y. S. Kivshar, "Nonradiating anapole modes in dielectric nanoparticles," Nat. Commun. **6**(1), 8069 (2015).
20. B. Ögüt, N. Talebi, R. Vogelgesang, W. Sigle, and P. A. van Aken, "Toroidal plasmonic eigenmodes in oligomer nanocavities for the visible," Nano Lett. **12**(10), 5239–5244 (2012).
21. A. A. Basharin, M. Kafesaki, E. N. Economou, C. M. Soukoulis, V. A. Fedotov, V. Savinov, and N. I. Zheludev, "Dielectric metamaterials with toroidal dipolar response," Phys. Rev. X **5**(1), 011036 (2015).
22. L. Wei, Z. Xi, N. Bhattacharya, and H. P. Urbach, "Excitation of the radiationless anapole mode," Optica **3**(8), 799–802 (2016).
23. A. A. Basharin, V. Chuguevsky, N. Volsky, M. Kafesaki, and E. N. Economou, "Extremely high Q-factor metamaterials due to anapole excitation," Phys. Rev. B **95**(3), 035104 (2017).
24. J. S. T. Gongora, A. E. Miroshnichenko, Y. S. Kivshar, and A. Fratalocchi, "Anapole nanolasers for mode-locking and ultrafast pulse generation," Nat. Commun. **8**(1), 15535 (2017).
25. B. Luk'yanchuk, R. Paniagua-Domínguez, A. I. Kuznetsov, A. E. Miroshnichenko, and Y. S. Kivshar, "Suppression of scattering for small dielectric particles: anapole mode and invisibility," Phil. Trans. R. Soc. A **375**(2090), 20160069 (2017).
26. P. C. Wu, C. Y. Liao, V. Savinov, T. L. Chung, W. T. Chen, Y. W. Huang, P. R. Wu, Y. H. Chen, A. Q. Liu, N. I. Zheludev, and D. P. Tsai, "Optical Anapole Metamaterial," ACS Nano **12**(2), 1920–1927 (2018).
27. K. V. Baryshnikova, D. A. Smirnova, B. S. Luk'yanchuk, and Y. S. Kivshar, "Optical anapoles: concepts and applications," Adv. Opt. Mater. **7**(14), 1801350 (2019).
28. N. Pavlov, I. Stenishchev, A. Ospanova, P. Belov, P. Kapitanova, and A. Basharin, "Toroidal dipole mode observation in situ," Phys. Status Solidi B **257**(3), 1900406 (2020).
29. K. E. Ballantine and J. Ruostekoski, "Radiative toroidal dipole and anapole excitations in collectively responding arrays of atoms," arXiv:2005.05918v1 (2020).
30. D. C. Zografopoulos, A. Ferraro, J. F. Algorri, P. Martín-Mateos, B. García-Cámara, A. Moreno-Oyervides, V. Krozer, P. Acedo, R. Vergaz, J. M. Sánchez-Pena, and R. Beccherelli, "All-dielectric silicon metasurface with strong subterahertz toroidal dipole resonance," Adv. Opt. Mater. **7**(19), 1900777 (2019).
31. D. C. Zografopoulos, J. F. Algorri, A. Ferraro, B. García-Cámara, J. M. Sánchez-Pena, and R. Beccherelli, "Toroidal metasurface resonances in microwave waveguides," Sci. Rep. **9**(1), 7544 (2019).
32. A. K. Ospanova, I. V. Stenishchev, and A. A. Basharin, "Anapole mode sustaining silicon metamaterials in visible spectral range," Laser Photonics Rev. **12**(7), 1870031 (2018).
33. J. F. Algorri, D. C. Zografopoulos, A. Ferraro, B. García-Cámara, R. Vergaz, R. Beccherelli, and J. M. Sánchez-Pena, "Anapole Modes in Hollow Nanocuboid Dielectric Metasurfaces for Refractometric Sensing," Nanomaterials **9**(1), 30 (2018).
34. N. A. Nemkov, A. A. Basharin, and V. A. Fedotov, "Nonradiating sources, dynamic anapole, and Aharonov-Bohm effect," Phys. Rev. B **95**(16), 165134 (2017).
35. N. A. Nemkov, I. V. Stenishchev, and A. A. Basharin, "Nontrivial nonradiating all-dielectric anapole," Sci. Rep. **7**(1), 1064 (2017).
36. V. A. Zenin, C. E. Garcia-Ortiz, A. B. Evlyukhin, Y. Yang, R. Malureanu, S. M. Novikov, V. Coello, B. N. Chichkov, S. I. Bozhevolnyi, A. V. Lavrinenko, and N. Asger Mortensen, "Engineering nanoparticles with pure high-order multipole scattering," ACS Photonics **7**(4), 1067–1075 (2020).
37. M. Gupta, Y. K. Srivastava, and R. Singh, "A toroidal metamaterial switch," Adv. Mater. **30**(4), 1704845 (2018).
38. L. Cong, V. Savinov, Y. K. Srivastava, S. Han, and R. Singh, "A metamaterial analog of the Ising model," Adv. Mater. **30**(40), 1804210 (2018).
39. M. Gupta and R. Singh, "Toroidal versus Fano resonances in high Q planar THz metamaterials," Adv. Opt. Mater. **4**(12), 2119–2125 (2016).

40. M. Gupta, V. Savinov, N. Xu, L. Cong, G. Dayal, S. Wang, W. Zhang, N. I. Zheludev, and R. Singh, “Sharp toroidal resonances in planar terahertz metasurfaces,” Adv. Mater. **28**(37), 8206–8211 (2016).
41. A. J. Devaney and E. Wolf, “Multipole expansions and plane wave representations of the electromagnetic field,” J. Math. Phys. **15**(2), 234–244 (1974).
42. L. D. Landau and E. Lifshitz, *The Classical Theory of Fields* (Butterworth-Heinemann, 1975).
43. J. D. Jackson, *Classical Electrodynamics* (Wiley, 1999).
44. R. E. Raab and O. L. De Lange, *Multipole Theory in Electromagnetism* (Clarendon, 2005).
45. V. M. Dubovik and V. V. Tugushev, “Toroid moments in electrodynamics and solid-state physics,” Phys. Rep. **187**(4), 145–202 (1990).
46. E. E. Radescu and G. Vaman, “Exact calculation of the angular momentum loss, recoil force, and radiation intensity for an arbitrary source in terms of electric, magnetic, and toroid multipoles,” Phys. Rev. E **65**(4), 046609 (2002).
47. Y. Yang and S. I. Bozhevolnyi, “Nonradiating anapole states in nanophotonics: from fundamentals to applications,” Nanotechnology **30**(20), 204001 (2019).
48. V. Savinov, N. Papasimakis, D. P. Tsai, and N. I. Zheludev, “Optical anapoles,” Commun. Phys. **2**(1), 69 (2019).
49. B. Luk’yanchuk, R. Paniagua-Domınguez, A. I. Kuznetsov, A. E. Miroshnichenko, and Y. S. Kivshar, “Hybrid anapole modes of high-index dielectric nanoparticles,” Phys. Rev. A **95**(6), 063820 (2017).
50. E. A. Gurvitz, K. S. Ladutenko, P. A. Dergachev, A. B. Evlyukhin, A. E. Miroshnichenko, and A. S. Shalin, “The high-order toroidal moments and anapole states in all-dielectric photonics,” Laser Photonics Rev. **13**(5), 1800266 (2019).
51. C. Vrejoiu, “Electromagnetic multipoles in Cartesian coordinates,” J. Phys. A: Math. Gen. **35**(46), 9911–9922 (2002).
52. N. A. Nemkov, A. A. Basharin, and V. A. Fedotov, “Electromagnetic sources beyond common multipoles,” Phys. Rev. A **98**(2), 023858 (2018).
53. B. Luk’yanchuk, N. Voshchinnikov, R. Paniagua-Dominguez, and A. Kuznetsov, “Optimum forward light scattering by spherical and spheroidal dielectric nanoparticles with high refractive index,” ACS Photonics **2**(7), 993–999 (2015).
54. B. T. Draine, “Interstellar Dust Grains,” Annu. Rev. Astron. Astrophys. **41**(1), 241–289 (2003).
55. N. V. Voshchinnikov, V. B. Il’in, and T. Henning, “Modelling the optical properties of composite and porous interstellar grains,” Astron. Astrophys. **429**(2), 371–381 (2005).
56. R. Siebenmorgen, N. V. Voshchinnikov, and S. Bagnulo, “Dust in the diffuse interstellar medium - Extinction, emission, linear and circular polarization,” Astron. Astrophys. **561**, A82 (2014).
57. R. Siebenmorgen, N. V. Voshchinnikov, S. Bagnulo, and N. L. J. Cox, “Constraints on interstellar dust models from extinction and spectro-polarimetry,” Planet. Space Sci. **149**, 64–71 (2017).
58. V. Savinov, “Novel toroidal and superconducting metamaterials,” Ph.D. thesis. University of Southampton (2014).
59. A. C. Valero, E. A. Gurvitz, F. A. Benimetskiy, A. Samusev, M. Rahmani, K. Z. Kamali, A. B. Evlyukhin, A. A. Pavlov, A. E. Miroshnichenko, and A. S Shalin, “Nontrivial pure zero-scattering regime delivered by a hybrid anapole state,” arXiv:2004.04659 (2020).
60. A. Monti, A. Toscano, and F. Bilotti, “Analysis of the scattering and absorption properties of ellipsoidal nanoparticle arrays for the design of full-color transparent screens,” J. Appl. Phys. **121**(24), 243106 (2017).
61. H. Deng, P. Dutta, and J. Liu, “Entry modes of ellipsoidal nanoparticles on a membrane during clathrin-mediated endocytosis,” Soft Matter **15**(25), 5128–5137 (2019).
62. B. V. K. J. Schmidt, C. X. Wang, S. Kraemer, L. A. Connal, and D. Klinger, “Highly functional ellipsoidal block copolymer nanoparticles: a generalized approach to nanostructured chemical ordering in phase separated colloidal particles,” Polym. Chem. **9**(13), 1638–1649 (2018).
63. P. Desai, A. Venkataramanan, R. Schneider, M. K. Jaiswal, J. K. Carrow, A. Purwada, A. Singh, and A. K. Gaharwar, “Self-assembled, ellipsoidal polymeric nanoparticles for intracellular delivery of therapeutics,” J. Biomed. Mater. Res. **106**(7), 2048–2058 (2018).
64. D. A. Pawlak, K. Kolodziejak, S. Turczynski, J. Kisielewski, K. Rożniatowski, R. Diduszko, M. Kaczkan, and M. Malinowski, “Self-organized, rodlike, micrometer-scale microstructure of $Tb_3Sc_2Al_3O_{12}-TbScO_3$:Pr eutectic,” Chem. Mater. **18**(9), 2450–2457 (2006).
65. E. Ben-Akiva, R. A. Meyer, H. Yu, J. T. Smith, D. M. Pardoll, and J. J. Green, “Biomimetic anisotropic polymeric nanoparticles coated with red blood cell membranes for enhanced circulation and toxin removal,” Sci. Adv. **6**(16), eaay9035 (2020).
66. A. A. Basharin, M. Kafesaki, E. N. Economou, and C. M. Soukoulis, “Backward wave radiation from negative permittivity waveguides and its use for THz subwavelength imaging,” Opt. Express **20**(12), 12752–12760 (2012).
67. M. Massaouti, A. A. Basharin, M. Kafesaki, M. F. Acosta, R. I. Merino, V. M. Orera, E. N. Economou, C. M. Soukoulis, and S. Tzortzakis, “Eutectic epsilon-near-zero metamaterial terahertz waveguides,” Opt. Lett. **38**(7), 1140–1142 (2013).
68. V. Myroshnychenko, A. Stefanski, A. Manjavacas, M. Kafesaki, R. I. Merino, V. M. Orera, D. A. Pawlak, and F. J. G. de Abajo, “Interacting plasmon and phonon polaritons in aligned nano- and microwires,” Opt. Express **20**(10), 10879–10887 (2012).
69. D. A. Pawlak, S. Turczynski, M. Gajc, K. Kolodziejak, R. Diduszko, K. Rozniatowski, J. Smalc, and I. Vendik, “How far are we from making metamaterials by self-organization? the microstructure of highly anisotropic particles with an SRR-like geometry,” Adv. Funct. Mater. **20**(7), 1116–1124 (2010).
70. X. Cui, Y. Lai, R. Ai, H. Wang, L. Shao, H. Chen, W. Zhang, and J. Wang, “Anapole states and toroidal resonances realized in simple gold nanoplate-on-mirror structures,” Adv. Opt. Mater. **2020**, 2001173 (2020).